Hindawi
Advances in Civil Engineering
Volume 2020, Article ID 8890562, 12 pages
https://doi.org/10.1155/2020/8890562

Research Article

An Experimental Investigation on Dynamic Characteristics of Soft Soils Treated by Vibration-Drainage Method

Jie Yin, Yong Tang, Yong-hong Miao, and Ruo-yu Sheng

Department of Civil Engineering, Faculty of Civil Engineering and Mechanics, Jiangsu University, Zhenjiang 212013, China

Correspondence should be addressed to Jie Yin; yinjie@ujs.edu.cn

Received 23 June 2020; Revised 9 August 2020; Accepted 14 August 2020; Published 29 August 2020

Academic Editor: Qiang Tang

This paper presents an experimental investigation on the dynamic characteristics of soft soils that are treated by vibration-drainage method (VDM). The representative dynamic axial strain at a given number of cycles was obtained. The VDM-treated soft soil exhibited different dynamic deformation characteristics that are not only affected by the cyclic frequency but also influenced by the vibration frequency during the treatment process. Soil specimens at different cyclic frequencies show a similar variation trend that the axial strain systematically grows with increasing number of cycles. The rate of axial strain for all specimens systematically linearly decreases with the increase of number of cycles in the log-log scale. Results showed that both axial strain and strain rate exhibit relatively lower values at a given number of cycles under the condition that the applied cyclic frequency is equal to vibration frequency. It is expected that the soil structure will be more stable if the applied cyclic frequency is close to the vibration frequency that is applied on VDM-treated soil. Therefore, the vibration frequency close to the possible dynamic loading frequency is recommended in the process of soft soil improvement via VDM in the related engineering applications.

1. Introduction

It has been well documented that the naturally deposited soft soil usually exhibits poor engineering properties such as poor permeability, high compressibility, and low strength [1, 2]. Therefore, the infrastructures that are built upon soft soil foundations will result in some unfavorable problems if the soft soil is not treated well [3]. To solve these problems, some common methods dealing with soft soils have been developed such as replacement method, compaction grouting, deep soil mixing, vacuum preloading, micro- or minipiles, dynamic compaction, and dynamic-static drainage consolidation [4–17].

Among these methods, the dynamic-static drainage consolidation is a newly developed soil improvement technique widely used in China, which combines the traditional dynamic compaction with the static consolidation method. The limitations of both individual methods can be overcome, where the dynamic compaction is inapplicable to soft clay and a long time is spent on the water drainage during the static consolidation process. It should be noted that the traditional dynamic compaction usually uses an impact load with hammer tamping that results in some unfavorable issues with soft soils such as excessive lateral deformation, extrusion failure, and rubber soil [18–21]. An improved method has been provided to address the above issues by applying a vibration load to replace the impact load [22, 23]. Additionally, a vertical drainage system was set to accelerate the water drainage under the vibration load, named as the vibration-drainage method (VDM). This method was inspired by the principle of vibration oil recovery [24–26], which can accelerate solid and liquid separation. Previous works have shown that the VDM-treated soils exhibit favorable mechanical properties which can be used in various engineering applications such as highway engineering and costal engineering [27].

It should be noted that those treated soft soil foundations might still be subject to the effects of some dynamic loads such as highway traffic load, tidal water-level changes, and shore wave action. For further evaluating the dynamic characteristics of soft soils if treated by VDM, a series of laboratory tests were conducted on VDM-treated soft soil

specimens considering the effect of the frequency applied on the soft soil specimens prepared in and after the VDM treatment process. Recommendations have been suggested in the geotechnical applications on soft soils treated by the vibration-drainage method.

2. Materials and Methods

2.1. Materials. Soft soil samples used in this study were acquired from an engineering site in Lianyungang city of China. The in situ water content of the soil sample was 45.2% as per ASTM D2216 [28]. The plastic limit (PL) and liquid limit (LL) were 21 and 43 according to ASTM D4318 [29], respectively. The corresponding plasticity index (PI = LL-PL) is 22. The specific gravity (G_s) of the soil sample was 2.68 measured following ASTM D854 [30]. According to the Unified Soil Classification System [31], the sample belongs to lean clay (CL).

2.2. Methods. A portable mechanical mixer was used to blend the soil sample obtained from the field by adding water with a target water content of approximately 64.5% (about 1.5 times the liquid limit). After blending, the slurry-like mixture was poured into a cylindrical specimen mold (inner diameter $D = 61.8$ mm and height $H = 130$ mm) to prepare the untreated soil specimen. Four geotextile filter strips (with length = 15 cm and width = 1.5 cm) were evenly distributed along the inner wall of the specimen mold as the vertical drainage system.

A vibration loading system (Figure 1) developed in the previous study [23] was used herein to prepare the VDM-treated soil specimen. Each untreated soil specimen was isotropically consolidated under 100 kPa for 24 h, reflecting the influence of surrounding pressure on the soil. Because of the low strength of the test soft soil, the direct application of large load or vibration load easily causes the failure of the test. A target vertical static load of 0.2 kN was applied incrementally three times onto the soil specimen (i.e., 0.067 kN for each load increment). A sinusoidal harmonic vibration loading was thereafter applied onto the soil specimen with different vibration frequencies (f_v) from 0 Hz to 5 Hz (i.e., 0 Hz, 1 Hz, 2 Hz, and 5 Hz). The total loading process lasted for 400 min for each specimen under drained condition. After the static and dynamic loading process, specimens were taken out of the chamber in Figure 1. Each specimen was then carefully trimmed to prepare the VDM-treated specimen with a cylindrical size of $D = 39.1$ mm and $H = 80$ mm. The VDM-treated specimens were used for the following undrained dynamic triaxial loading tests in the DSZ-2 dynamic triaxial instrument, as shown in Figure 2.

Table 1 shows the detailed testing program for the untreated and VDM-treated soil specimens. For untreated soil specimens, the confining pressure (σ_3') applied to the specimen is 100 kPa. The static load of 0.2 kN was applied incrementally onto the soil with three loading increments. A sinusoidal harmonic vibration load of 0.05 kN was thereafter applied onto the soil specimen with different frequencies as mentioned above (i.e., 0 Hz, 1 Hz, 2 Hz, and 5 Hz). For the VDM-treated soil specimen, the confining pressure (σ'_3) was set as 100 kPa and the dynamic stress of 40 kPa was applied with cyclic frequencies (f_c) of 1 Hz, 2 Hz, and 5 Hz, which are consistent with the vibration frequencies.

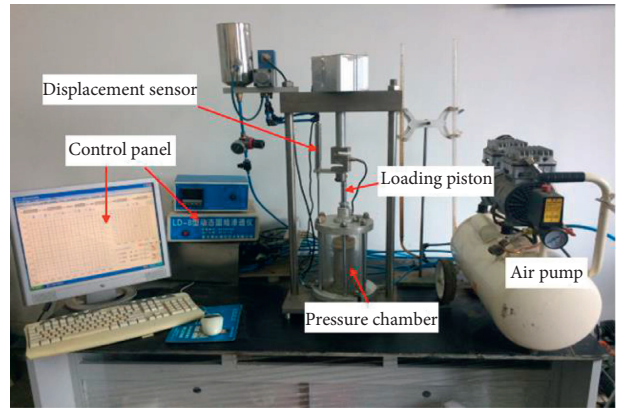

Figure 1: Photograph of the cyclic loading system.

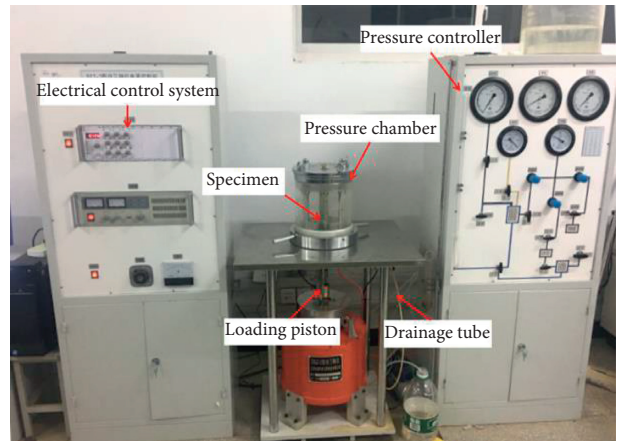

Figure 2: Photograph of the DSZ-2 dynamic triaxial instrument.

3. Results

3.1. Vibration Drainage Behavior of Untreated Soils. For untreated soil specimens, the vibration load was applied with various values of frequency from 0 Hz to 5 Hz. Figures 3 and 4 show the results obtained from vibration drainage tests. Figure 3 shows the variation of cumulative drainage volume with time for specimens under different vibration frequencies. It can be seen that the vibration frequency (f_v) has a significant effect on the cumulative drainage volume during the treatment process. Cumulative drainage volume increases significantly at a relatively earlier time for all specimens and tends to be stable when the time continues to increase. Results show that the specimen under vibration load exhibits higher drainage volume than that under static load at a given time. The possible reason is that cyclic shear stresses will result in the generation of excess pore pressures due to the low permeability of soft soils [32]. Besides, the specimen at $f_v = 1$ Hz shows the largest cumulative drainage volume compared with that at $f_v = 2$ and 5 Hz. This is because

Table 1: Testing program.

Untreated soil specimen ($D = 61.8$ mm, $H = 130$ mm)				VDM-treated soil specimen ($D = 39.1$ mm, $H = 80$ mm)			No. of tests
Confining pressure, σ_3' (kPa)	Value of static load (kN)	Value of vibration load (kN)	Vibration frequency, f_v (Hz)	Confining pressure, σ_3' (kPa)	Dynamic stress (kPa)	Cyclic frequency, f_c (Hz)	
100	0.2	—	0	100	40	1, 2, 5	3
100	0.2	0.05	1	100	40	1, 2, 5	3
100	0.2	0.05	2	100	40	1, 2, 5	3
100	0.2	0.05	5	100	40	1, 2, 5	3

the applied vibration loads at $f_v = 1$ Hz are close to the soil's natural frequency. The resonant effect will drive the soil specimen to oscillate with greater amplitude and enable more water to drain out from the soil specimen [23]. Figure 4 shows the total cumulative drainage volume with vibration frequency. It also shows the vibration frequency-dependent characteristics, and a maximum value of the volume of 11.6 mL can be observed when $f_v = 1$ Hz.

Figures 5 and 6 show the results of axial strain obtained from vibration drainage tests. Figure 5 shows the variation of axial strain with time, and the trends are similar to that of cumulative drainage volume with time, as shown in Figure 3. It can be observed that the axial strain grows remarkably at a relatively shorter time and tends to be stable as the time continues to increase. The axial strain-time curves for specimens under vibration load all lie above that for specimens under static load, which is consistent with the variation of cumulative drainage volume with time. Specifically, the specimen under 1 Hz shows the highest axial strain at a certain time, which is comparable with the largest cumulative drainage volume at $f_v = 1$ Hz, as shown in Figure 3. It is expected that under the same confining pressure, the larger the drainage volume is, the bigger the axial strain is. Figure 6 shows the variation of total final axial strain with vibration frequency, and it can be observed that the final axial strain shows the maximum value of 6.8% when $f_v = 1$ Hz.

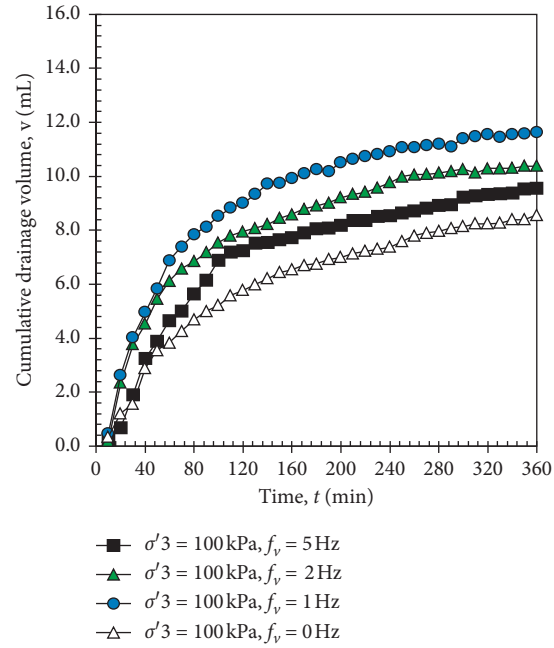

Figure 3: Variation of cumulative drainage volume with time.

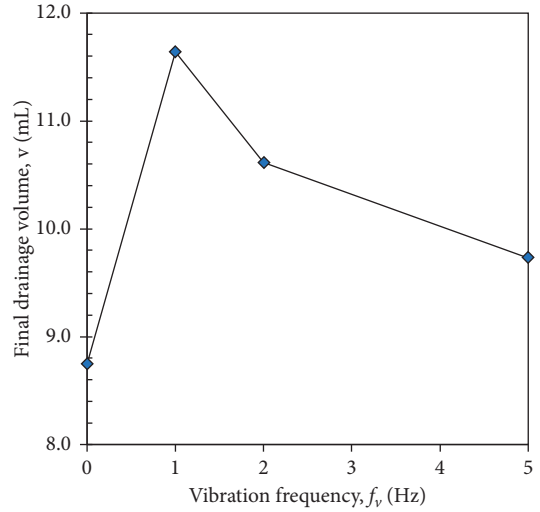

Figure 4: Variation of final drainage volume with vibration frequency.

3.2. Results of Dynamic Triaxial Test. To further investigate the dynamic characteristics of VDM-treated soils at different vibration frequencies (f_v), the dynamic triaxial tests under undrained conditions at different cyclic frequencies (f_c) of 1 Hz, 2 Hz, and 5 Hz were conducted on VDM-treated soil specimens. Following the testing program listed in Table 1, the axial strain as a function of the number of cycles can be obtained for VDM-treated specimens. For example, Figure 7 shows the two sets of raw data of ε_a-N for VDM-treated soil specimens at $f_c = 1$ Hz and $f_v = 0$ and 1 Hz in dynamic triaxial tests. Since some parts of the row data overlapped, they can be simplified using some representative data points, as shown in Figure 8. The ε_a-N curve in each cycle can be processed through the following equation to yield a value of ε_{aN}:

$$\varepsilon_{aN} = \frac{\varepsilon_{\max N} + \varepsilon_{\min N}}{2}, \quad (1)$$

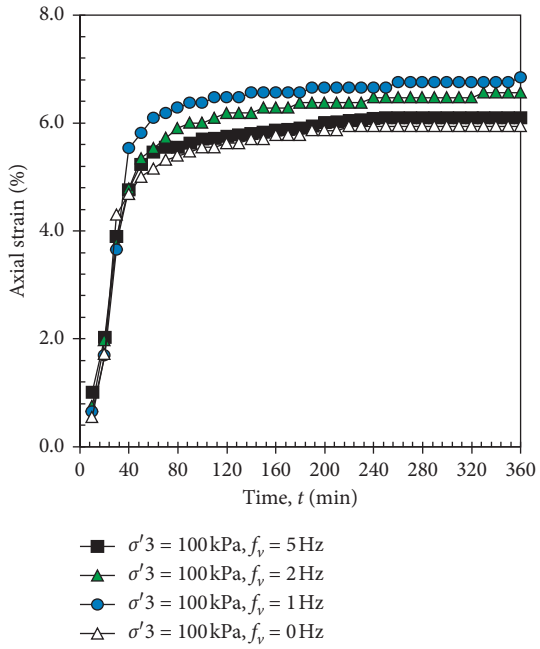

Figure 5: Variation of axial strain with time.

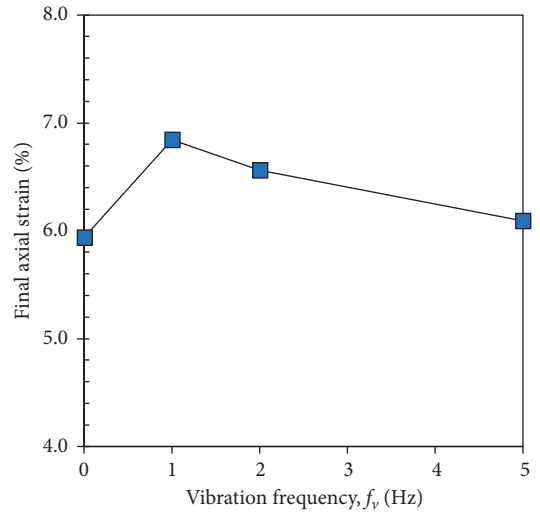

Figure 6: Variation of final axial strain with vibration frequency.

where ε_{aN} is the axial strain at the N^{th} cycle and $\varepsilon_{\max N}$ and $\varepsilon_{\min N}$ are the maximum and minimum of axial strains at the cycles of N. By connecting the data point with respect to the value of ε_{aN} and N, a simplified representative red line can be obtained as shown in Figure 8. Similar simplification methods have also been reported in the existing literature [3, 33, 34].

3.2.1. Effect of Cyclic Frequency. In order to evaluate the effect of cyclic frequency f_c on dynamic deformation behavior of VDM-treated soft soil, Figure 9 shows the variation of axial strain ε_a with the number of cycles N for soil specimens at various f_c (i.e., 1 Hz, 2 Hz, and 5 Hz) at a given f_v. Figure 9(a) shows the scenario of $f_v = 0$ as a reference

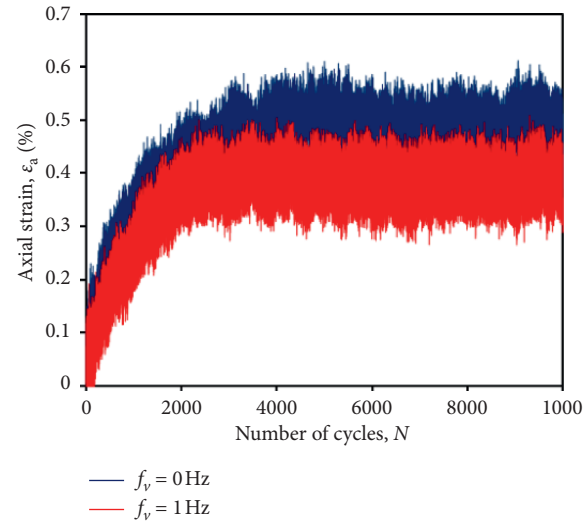

Figure 7: Variation of axial strain with the number of cycles for VDM-treated soil specimens at $f_c = 1$ Hz.

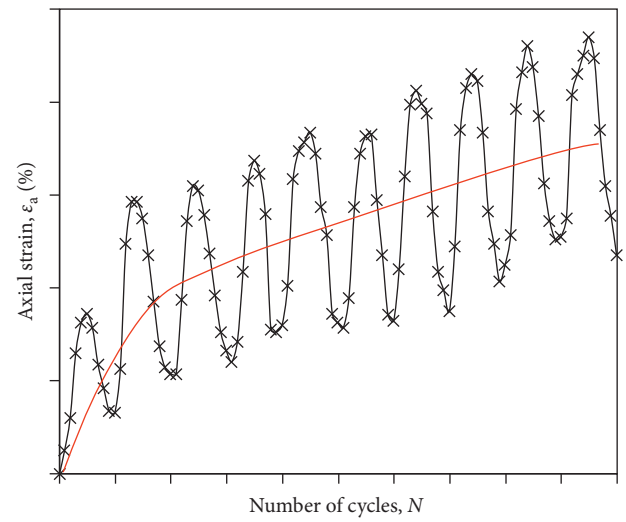

Figure 8: The simplified treatment schematic.

reflecting the soil specimens treated by static load compared with $f_v = 1$ Hz, 2 Hz, and 5 Hz in Figures 9(b)–9(d), respectively.

It can be seen in Figure 9(a) that soil specimens under different f_c show a similar variation trend in terms of ε_a and N, i.e., ε_a increases with increasing N. The ε_a-N curve at higher f_c lies below that at lower f_c, indicating that f_c has a significant effect on ε_a for specimens treated under static load ($f_v = 0$). This is because when the dynamic load (40 kPa in this study) is less than the "safe load" (under which the strain of soil specimen increases very slowly), the soil structure will be more stable under the higher frequency dynamic load [34–36].

Figures 9(b) to 9(d) show the results of ε_a-N curves at various f_c for VDM-treated soil specimens at different vibration frequencies. A similar increasing trend of ε_a with N can be seen compared with the static load results in Figure 9(a). In general, ε_a-N curve at higher f_c lies below that

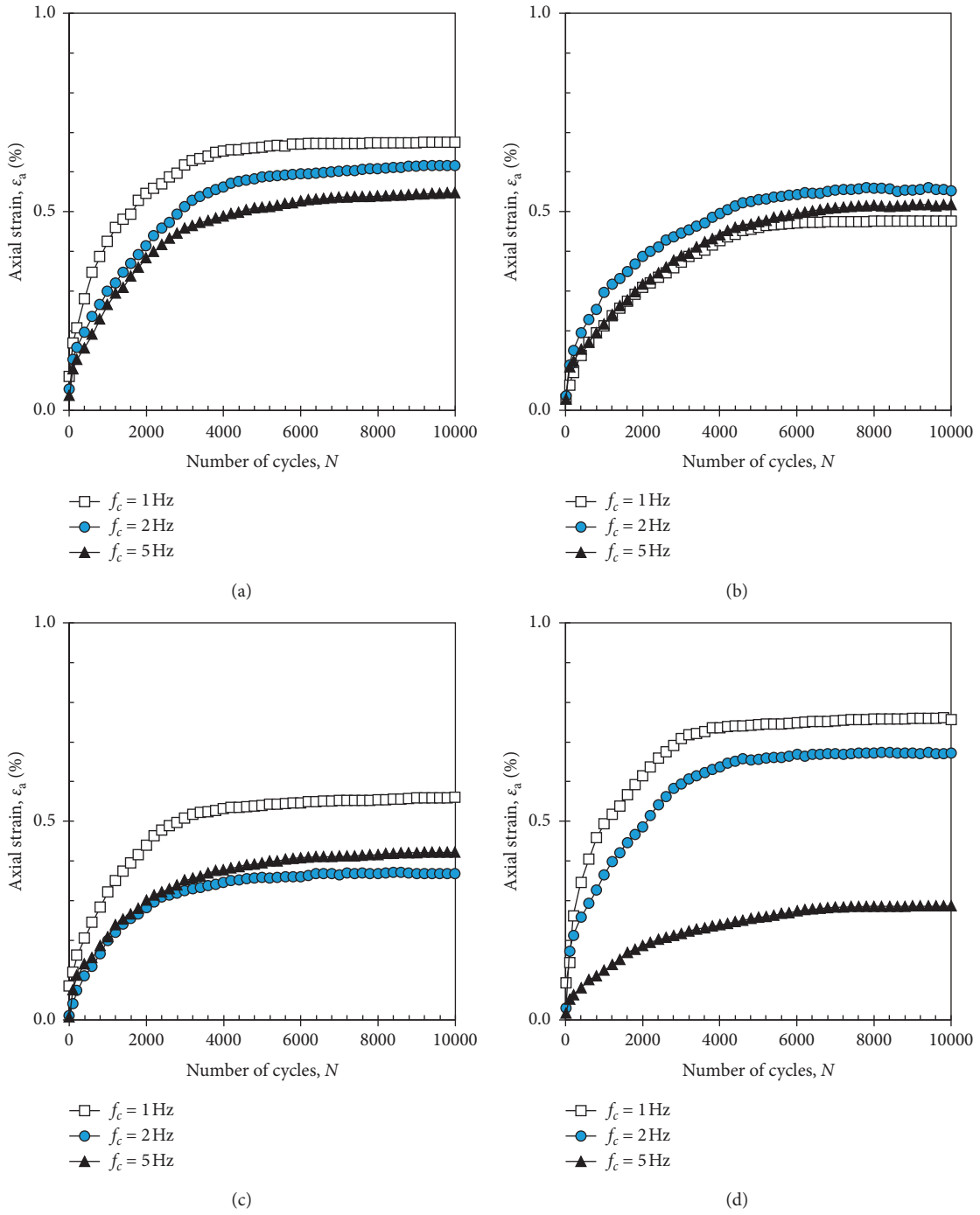

Figure 9: Variation of ε_a with N on VDM-treated specimens at f_v of (a) 0 Hz, (b) 1 Hz, (c) 2 Hz, and (d) 5 Hz.

at lower f_c except for a case. The difference is that when $f_v = f_c$, the ε_a-N curve is lying on the bottom indicating the soil structure is more stable. It means that the vibration frequency f_v during the VDM-treated process can affect the deformation behavior of VDM-treated soil at different f_c.

For further investigating the effect of f_c on axial strain rate $\dot{\varepsilon}_a$, test data in Figure 9 were used to determine $\dot{\varepsilon}_a$ at a given number of cycles N for VDM-treated soil specimens at various f_c (i.e., 1 Hz, 2 Hz, and 5 Hz), and the results are shown in Figure 10. Figure 10(a) depicts the variation of $\dot{\varepsilon}_a$ with N for specimens treated under static load ($f_v = 0$). It can be seen that $\dot{\varepsilon}_a$-N curves for specimens treated at different f_c show a consistent linearly decreasing trend in the log-log scale. Moreover, the $\dot{\varepsilon}_a$-N curve of the specimen at higher f_c lies above that of the specimen at lower f_c. The reason is that the specimen at a higher f_c will take less time to reach the same cycles. It can be seen in Figure 11 that axial strain at a higher f_c takes less time to increase, resulting in a higher value of $\dot{\varepsilon}_a$.

In contrast, Figures 10(b) to 10(d) show the axial strain rate $\dot{\varepsilon}_a$ as a function of the number of cycles N for specimens treated at the vibration loading frequency $f_v = 1$ Hz, 2 Hz,

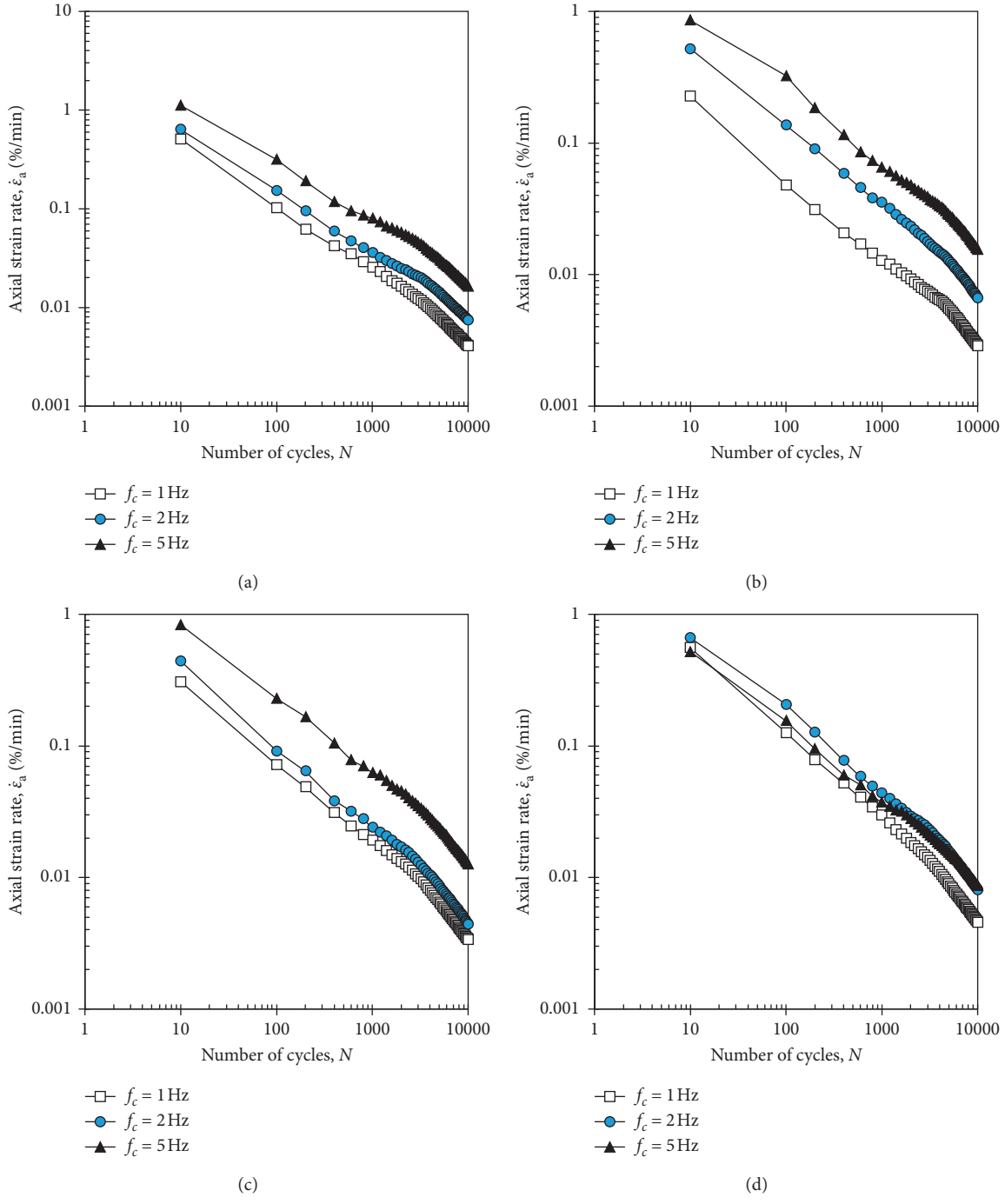

Figure 10: Variation of $\dot{\varepsilon}_a$ with N at f_v of (a) 0 Hz, (b) 1 Hz, (c) 2 Hz, and (d) 5 Hz.

and 5 Hz, respectively. A similar variation trend of $\dot{\varepsilon}_a$ with N can be observed as $\dot{\varepsilon}_a$ linearly decreases with increasing N compared with the results in Figure 10(a). The same feature can also be observed in Figure 10(d) that, at a given f_v, the higher the f_c, the greater the value of $\dot{\varepsilon}_a$ at a certain N except for $f_c = 5$ Hz. It can be found that the $\dot{\varepsilon}_a$-N curve for the specimen at $f_c = 5$ Hz lies below the curve for the specimen at $f_c = 2$ Hz. According to Figure 11(d), the significantly lower axial strain at $f_c = 5$ Hz caused the phenomenon. This is possibly caused by the fact that the soil structure had undergone the vibration loading treatment at $f_v = 5$ Hz, so that the soil structure can maintain a relatively stable state under this frequency of vibration. When the dynamic cyclic loading frequency f_c is equal to f_v, the specimen would be more difficult to deform. Moreover, it can be found that the value of $\dot{\varepsilon}_a$ is different at the same N and f_c but different f_v. This indicates that the effect of f_v cannot be ignored, which will be further discussed in the next section.

In order to further evaluate the effect of f_c on the axial strain ε_a and axial strain rate $\dot{\varepsilon}_a$, the values of ε_a and $\dot{\varepsilon}_a$ at

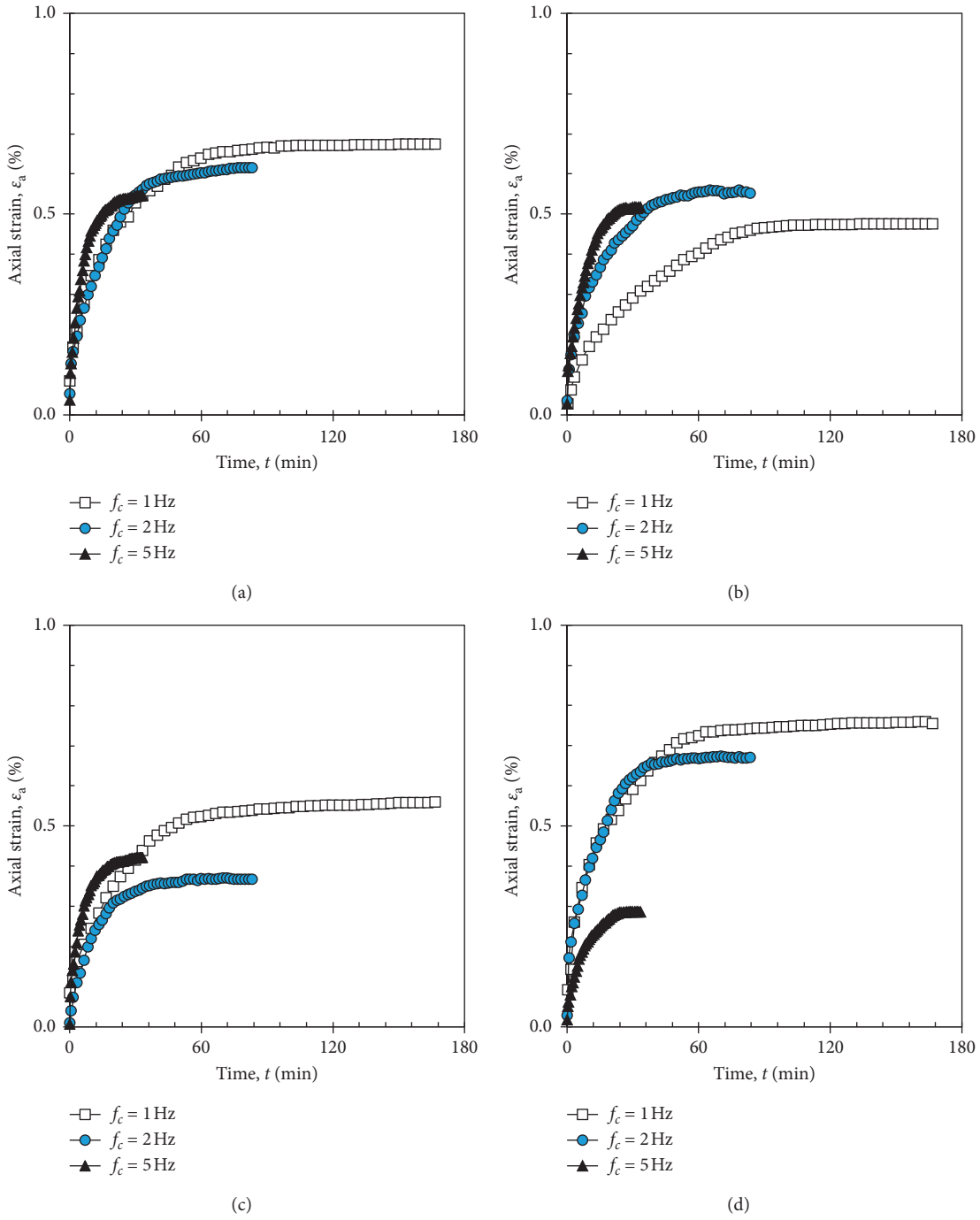

Figure 11: Variation of ε_a with t on VDM-treated specimens at f_v of (a) 0 Hz, (b) 1 Hz, (c) 2 Hz, and (d) 5 Hz.

$N = 10{,}000$ obtained from Figures (9) and (10) were replotted as a function of cyclic frequency f_c in Figures 12(a) and 12(b), respectively. It can be seen from Figure 12(a) that the value of ε_a at $N = 10{,}000$ almost decreases with the increase of f_c except for a little increase in ε_a from $f_c = 1$ to 2 Hz at $f_v = 1$ Hz and from $f_c = 2$ to 5 Hz at $f_v = 2$ Hz. Specifically, at a given f_v, a minimum value of ε_a can be found when the applied f_c is equal to f_v for specimens treated by vibration loading. In detail, a minimum value of $\varepsilon_a = 0.48\%$ when $f_c = f_v = 1$ Hz, a minimum value of $\varepsilon_a = 0.37\%$ when $f_c = f_v = 2$ Hz, and a minimum value of $\varepsilon_a = 0.29\%$ when $f_c = f_v = 5$ Hz were observed. These phenomena further indicated that the soil structure of VDM-treated soil specimens is more stable when $f_c = f_v$. Figure 12(b) depicts the variation of $\dot{\varepsilon}_a$ at $N = 10{,}000$ with f_c at different values of f_v. It can be seen that the value of $\dot{\varepsilon}_a$ at $N = 10{,}000$ significantly increases with increasing f_c for specimens at a given f_v except for a little increase in ε_a from $f_c = 1$ to 2 Hz at $f_v = 2$ Hz and from $f_c = 2$ to 5 Hz at $f_v = 5$ Hz. A similar phenomenon can be found in Figure 12(b) that a minimum value of $\dot{\varepsilon}_a$ at

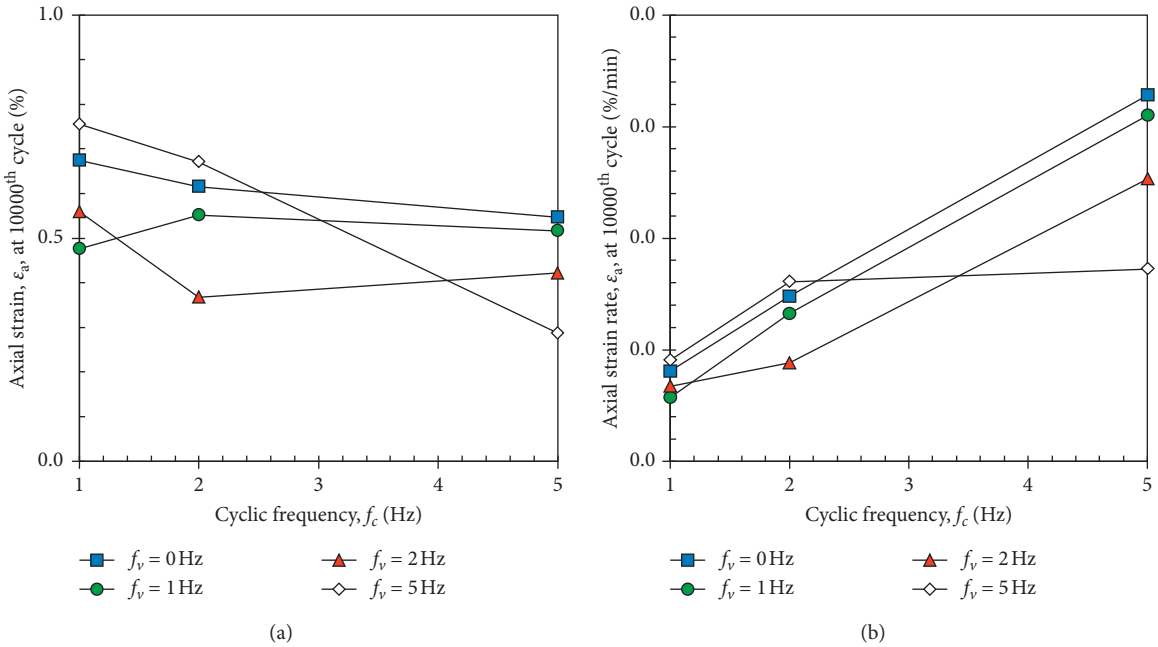

Figure 12: Variation of (a) ε_a and (b) $\dot{\varepsilon}_a$ with f_c at 10,000th cycle.

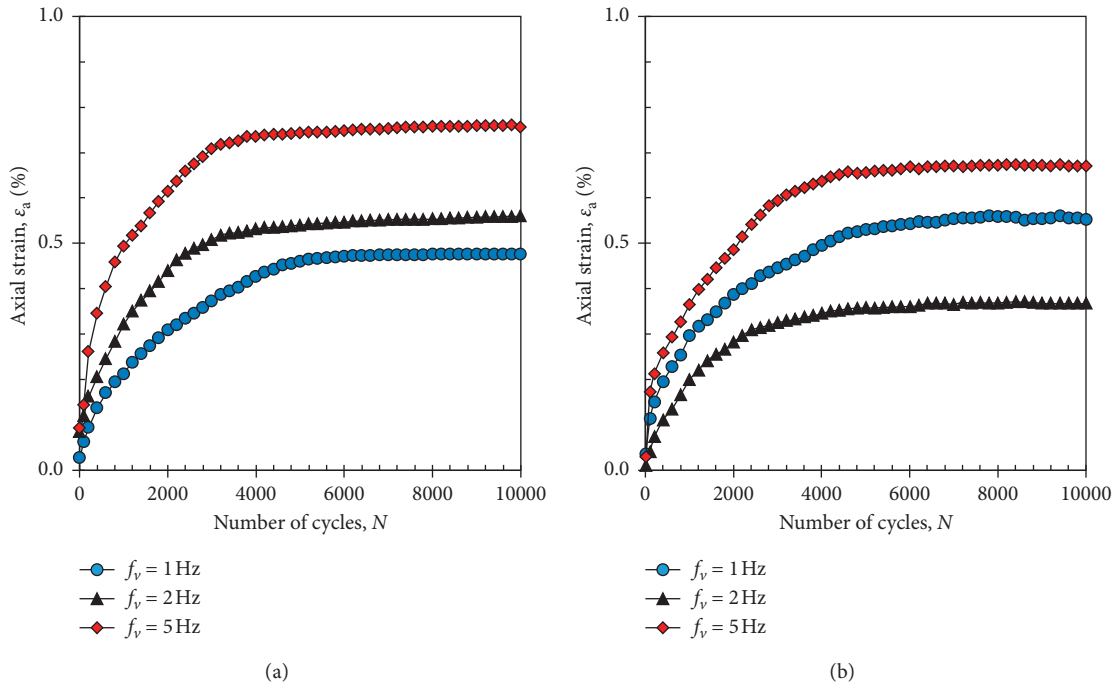

Figure 13: Continued.

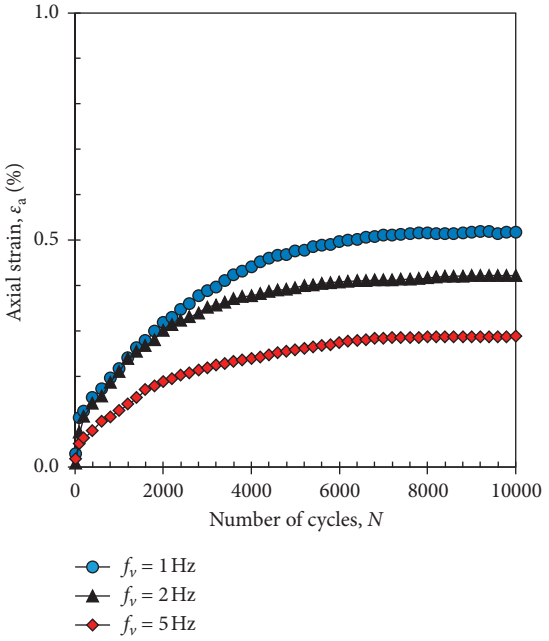

(c)

Figure 13: Variation of ε_a with N at f_c of (a) 1 Hz, (b) 2 Hz, and (c) 5 Hz.

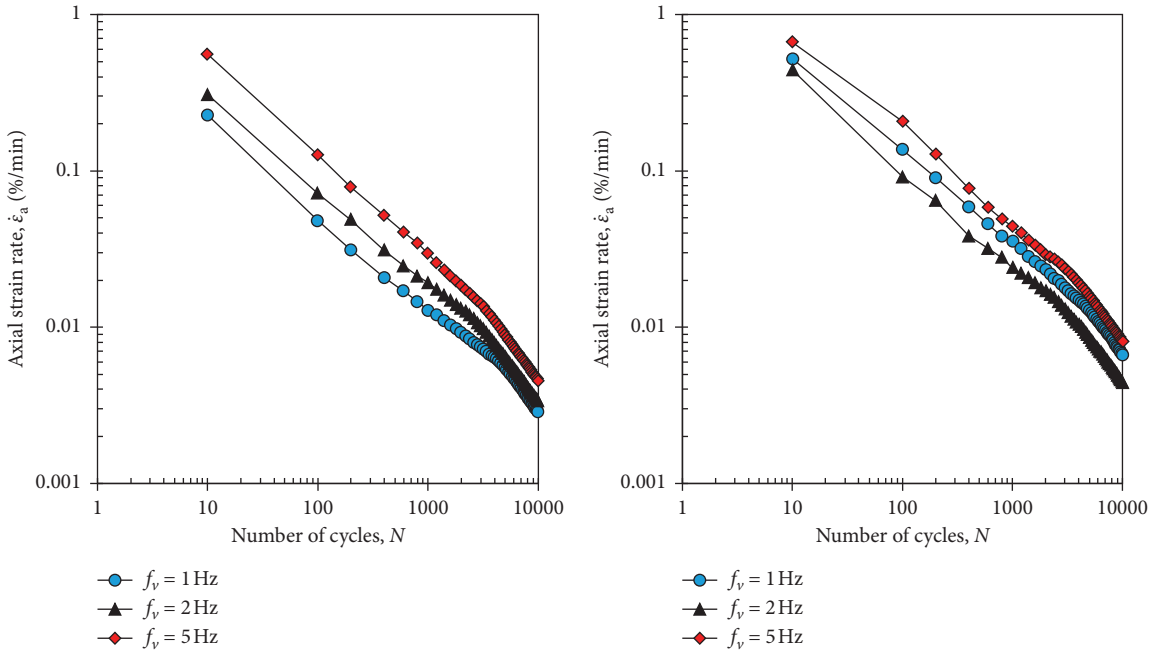

(a) (b)

Figure 14: Continued.

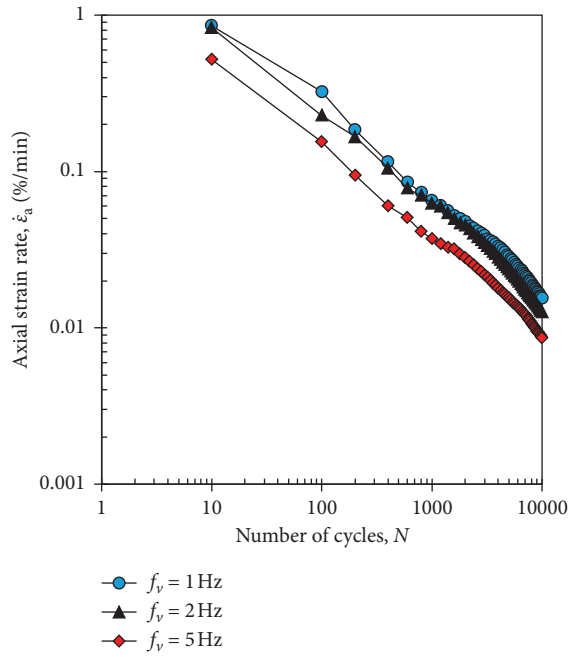

(c)

Figure 14: Variation of $\dot{\varepsilon}_a$ with N at f_c of (a) 1 Hz, (b) 2 Hz, and (c) 5 Hz.

$N = 10{,}000$ is obtained at a given f_c when $f_c = f_v$. In detail, i.e., a minimum value of $\dot{\varepsilon}_a = 0.0029\%/\text{min}$ at $f_c = f_v = 1$ Hz compared with $f_c = 1$ Hz and $f_v = 0$ Hz, 2 Hz, and 5 Hz, a minimum value of $\dot{\varepsilon}_a = 0.0044\%/\text{min}$ at $f_c = f_v = 2$ Hz, and a minimum value of $\dot{\varepsilon}_a = 0.0086\%/\text{min}$ at $f_c = f_v = 5$ Hz were observed. This also demonstrates that the soil structure for VDM-treated soil specimens is more stable when $f_c = f_v$.

3.2.2. Effect of Vibration Frequency. The above analysis indicated that VDM-treated soft soil exhibited different dynamic deformation characteristics not only affected by the cyclic frequency f_c but also influenced by the vibration frequency during the treatment process of VDM. For investigating the effect of f_v on dynamic deformation behavior of VDM-treated soft soil, Figure 13 depicts the variation of axial strain ε_a with the number of cycles N for soil specimens at various f_v (i.e., 1 Hz, 2 Hz, and 5 Hz) at a certain f_c. It can be observed in Figure 13 that ε_a consistently grows with the increase of N for specimens treated with different values of f_v. A significant increase in ε_a can be seen at a relatively lower magnitude of N (about 3000) and followed by a stable trend as N continues increasing. At a given N, the higher the value of f_v is, the higher the value of ε_a is, as shown in Figure 13(a). However, Figures 13(b) and 13(c) show different results. It can be found that the ε_a-N curve at $f_v = 2$ Hz lies at the bottom in Figure 13(b) yet the ε_a-N curve at $f_v = 5$ Hz lies at the bottom in Figure 13(c). The reason why the ε_a-N curve at different values of f_v did not follow the same trend is mainly due to the differences in the applied f_c. A similar result is that the ε_a-N curve always lies at the bottom when $f_v = f_c$. This result also demonstrates that the soil structure for VDM-treated soil specimens is more stable when $f_v = f_c$.

Figure 14 shows the variation of axial strain rate $\dot{\varepsilon}_a$ with the number of cycles N at different values of f_v in the log-log scale. It can be found that $\dot{\varepsilon}_a$ for all specimens systematically linearly decreases with the increase of N. Specifically, the $\dot{\varepsilon}_a$-N curve for specimens with applied f_v equal to f_c lies at the bottom resulting from the same reason as mentioned above. Therefore, it is expected that the soil structure will be more stable if the applied cyclic frequency is close to the vibration frequency using VDM treatment.

4. Conclusions

In this study, a series of laboratory tests were performed on VDM-treated soft soil specimens to investigate the dynamic characteristics of treated soils. Effects of the vibration frequency f_v applied in the treatment process and the cyclic frequency f_c applied on the treated soil specimens were evaluated, and the main conclusions are summarized below:

(1) Vibration frequency (f_v) has a significant effect on the cumulative drainage volume during the treatment process. Cumulative drainage volume increases significantly at a relatively earlier time for all specimens and tends to be stable when the time continues to increase. The specimen at $f_v = 1$ Hz shows the largest cumulative drainage volume.

(2) Soil specimens at different values of cyclic frequency (f_c) show a similar variation trend that the axial strain ε_a grows with increasing number of cycles. A

significant increase in ε_a was seen at a relatively lower N of about 3000 followed by a stable trend as N continues to increase. The axial strain rate ($\dot{\varepsilon}_a$) for all specimens systematically linearly decreases with the increase of N in the log-log scale.

(3) The influence of vibration frequency f_v cannot be ignored in the discussion of dynamic behavior of VDM-treated soil under cyclic load. At a given number of cycles N, both ε_a and $\dot{\varepsilon}_a$ show relatively lower values under the condition that the applied f_c is equal to f_v. It is expected that the soil structure will be less likely to settle and deform if the applied f_c is close to f_v.

Results from this study are based on Lianyungang soft soil from one source in China. However, a general trend is expected to be similar if specimens of soft soils from different sources are adopted. The VDM-treated soft soil exhibited different dynamic deformation characteristics not only affected by the cyclic frequency f_c but also influenced by the vibration frequency f_v during the treatment process. Results showed that soil structure will be more stable if the cyclic frequency of dynamic loads possibly applied to the foundation soil is equal to the vibration frequency used to treat the soft soil using the vibration-drainage method (VDM). Therefore, the vibration frequency should be carefully selected during the treatment process considering the possible value of cyclic frequency of dynamic load that may be encountered during the operation period. Vibration frequency close to the possible dynamic loading frequency is recommended in the process of soft soil improvement via VDM in related engineering applications.

Data Availability

Data are available from the corresponding author upon request.

Disclosure

The opinions, findings, conclusions, or recommendations expressed herein are those of the authors and do not necessarily represent the views of the sponsors.

Conflicts of Interest

The authors declare that they have no conflicts of interest.

Acknowledgments

The authors gratefully acknowledge the financial support from the National Natural Science Foundation of China (Grant no. 51978315).

References

[1] G. Xu, Y. Gao, J. Yin, R. Yang, and J. Ni, "Compression behavior of dredged slurries at high water contents," *Marine Georesources and Geotechnology*, vol. 33, no. 2, pp. 99–108, 2015.

[2] G. Xu and J. Yin, "Compression behavior of secondary clay minerals at high initial water contents," *Marine Georesources and Geotechnology*, vol. 34, no. 8, pp. 721–728, 2016.

[3] H. Lei, B. Li, H. Lu, and Q. Ren, "Dynamic deformation behavior and cyclic degradation of ultrasoft soil under cyclic loading," *Journal of Materials in Civil Engineering*, vol. 28, no. 11, Article ID 04016135, 2016.

[4] A. M. Amirebrahimi and L. R. Herrmann, "Continuum model and analysis of wick-drained systems," *International Journal for Numerical and Analytical Methods in Geomechanics*, vol. 17, no. 12, pp. 827–847, 1993.

[5] D. T. Bergado, T. Ruenkrairergsa, Y. Taesiri, and A. S. Balasubramaniam, "Deep soil mixing used to reduce embankment settlement," *Proceedings of the Institution of Civil Engineers - Ground Improvement*, vol. 3, no. 4, pp. 145–162, 1999.

[6] J. P. Carter, H. Sabetamal, M. Nazem, and S. W. Sloan, "One-dimensional test problems for dynamic consolidation," *Acta Geotechnica*, vol. 10, no. 1, pp. 173–178, 2015.

[7] Y. M. Chen, L. T. Zhan, X. J. Zhan, and W. A. Lin, "Field implementation of $FeCl_3$-conditioning and vacuum preloading for sewage sludge disposed in a sludge lagoon: a case study," *Geosynthetics International*, vol. 22, no. 4, pp. 327–338, 2015.

[8] J. Chu, S. W. Yan, and H. Yang, "Soil improvement by the vacuum preloading method for an oil storage station," *Géotechnique*, vol. 50, no. 6, pp. 625–632, 2000.

[9] N. N. Daud, Z. Yusoff, and A. Muhammed, "Ground improvement of problematic soft soils using shredded waste tyre," in *The Sixth Jordanian International Civil Engineering Conference (JICEC06)*, Amman, Jordan, March 2015.

[10] S. Hansbo, "Dynamic consolidation of mixed fill-a cost-effective alternative to piling: a case record," *Géotechnique*, vol. 46, no. 2, pp. 351–355, 1996.

[11] B. Indraratna, C. Rujikiatkamjorn, J. Ameratunga, and P. Boyle, "Performance and prediction of vacuum combined surcharge consolidation at port of brisbane," *Journal of Geotechnical and Geoenvironmental Engineering*, vol. 137, no. 11, pp. 1009–1018, 2011.

[12] M. Kitazume and M. Terashi, *The Deep Mixing Method*, CRC Press, Boca Raton, FL, UDA, 1st edition, 2013.

[13] A. H. Mahfouz, M. Gao, and M. Sharif, "Construction technology of modified vacuum pre-loading method for slurry dredged soil," *International Journal of Geological and Environmental Engineering*, vol. 10, no. 2, pp. 247–250, 2016.

[14] S. L. Shen, Z. F. Wang, S. Horpibulsuk, and Y. H. Kim, "Jet grouting with a newly developed technology: the twin-jet method," *Engineering Geology*, vol. 152, no. 1, pp. 87–95, 2013.

[15] Z. Sun, M. Gao, and W. Zhou, "Assessment of vacuum preloading of soft sediment applied to various drainage schemes," *Soil Mechanics and Foundation Engineering*, vol. 50, no. 6, pp. 255–261, 2014.

[16] S. W. Yan and J. Chu, "Soil improvement for a road using the vacuum preloading method," *Proceedings of the Institution of Civil Engineers - Ground Improvement*, vol. 7, no. 4, pp. 165–172, 2003.

[17] H. B. Zhang, X. G. Song, H. H. Wang, and Z. Ma, "Field test on the new method of vacuum dewatering with lower-energy dynamic consolidation for silty soil ground," *Advanced Materials Research*, vol. 243–249, pp. 3306–3310, 2011.

[18] L. J. Hua and L. Z Ming, "Soft soil improvement by static-dynamic drainage consolidation," *Soil Engineering and Foundation*, 2006.

[19] Y. K. Yang, W. Yang, and C. Y. Feng, "Experimental research of soft soil ground treatment in yangpu port by static-dynamic drainage consolidation," *Applied Mechanics and Materials*, vol. 353–356, pp. 203–207, 2013.
[20] J. Zhang and Y. Yang, "Research and application on soft soil foundation treatment by static-dynamic drainage consolidation," in *International Conference on Mechanic Automation and Control Engineering*, July 2011.
[21] L. J. Zhang, Z. M. Li, and K. T. Law, "Key factors for the dynamic-static drainage consolidation method," *Applied Mechanics and Materials*, vol. 105–107, pp. 827–831, 2011.
[22] Y. H. Miao, R. B. Li, and B. Chen, "Laboratory tests on consolidation behavior of soft soils under vibration drainage conditions," *Chinese Journal of Geotechnical Engineering*, vol. 38, no. 7, pp. 1301–1306, 2016, in Chinese.
[23] Y. H. Miao, F. B. Zhou, J. Yin, Y. C. Sun, R. B. Li, and J. F. Lu, "Effects of frequency and confining pressure on consolidation drainage behavior of soft marine clays," *Marine Georesources and Geotechnology*, vol. 37, no. 6, pp. 746–754, 2019.
[24] H. Jack, "Simulation oil production by wave energy," *World Oil*, no. 5, pp. 28–30, 2000.
[25] O. L. Kouznetsov, E. M. Simkin, G. V. Chilingar, and S. A. Katz, "Improved oil recovery by application of vibro-energy to waterflooded sandstones," *Journal of Petroleum Science and Engineering*, vol. 19, no. 3-4, pp. 191–200, 1998.
[26] O. R. Ganiev R, F. Ganiev L, and E. Ukrainsky, *Enhanced Oil Recovery: Resonance Macro- and Micro-mechanics of Petroleum Reservoirs*, Scrivener Publishing, Beverly, MA, USA, 2010.
[27] Y. H. Miao, R. Y. Sheng, J. Yin, F. B. Zhou, and J. F. Lu, "Dynamic characteristics of saturated soft clays under cyclic loading in drained condition," *KSCE Journal of Civil Engineering*, vol. 24, no. 2, pp. 443–450, 2020.
[28] ASTM, *Standard Test Methods for Laboratory Determination of Water (Moisture) Content of Soil and Rock by Mass. ASTM D2216-10*, ASTM, West Conshohocken, PA, USA, 2010a.
[29] ASTM, *Standard Test Methods for Liquid Limit, Plastic Limit, and Plasticity Index of Soils. ASTM 4318-10e1*, ASTM, West Conshohocken, PA, USA, 2010b.
[30] ASTM, *Standard Test Methods for Specific Gravity of Soil Solids by Water Pycnometer. ASTM D854-14*, ASTM, West Conshohocken, PA, USA, 2014c.
[31] ASTM, *Standard Practice for Classification of Soils for Engineering Purposes (Unified Soil Classification System). ASTM D2487-17*, ASTM, West Conshohocken, PA, USA, 2017.
[32] H. Yıldırım and H. Erşan, "Settlements under consecutive series of cyclic loading," *Soil Dynamics and Earthquake Engineering*, vol. 27, no. 6, pp. 577–585, 2007.
[33] J. Lu, B. Indraratna, X.-Y. Geng, J. P. Carter, and C. Rujikiatkamjorn, "Radial consolidation of soft soil under cyclic loads," *Computers and Geotechnics*, vol. 50, pp. 1–5, 2013.
[34] Q. Yang, Y. Tang, B. Yuan, and J. Zhou, "Cyclic stress-strain behaviour of soft clay under traffic loading through hollow cylinder apparatus: effect of loading frequency," *Road Materials and Pavement Design*, vol. 20, no. 5, pp. 1026–1058, 2018.
[35] Z. Cao, J. Chen, Y. Cai, L. Zhao, C. Gu, and J. Wang, "Long-term behavior of clay-fouled unbound granular materials subjected to cyclic loadings with different frequencies," *Engineering Geology*, vol. 243, pp. 118–127, 2018.
[36] H. Lei, J. Liu, M. Liu, Z. Zhang, and M. Jiang, "Effects of frequency and cyclic stress ratio on creep behavior of clay under cyclic loading," *Marine Georesources and Geotechnology*, vol. 35, no. 2, pp. 281–291, 2017.